Braz J Phys (2012) 42:186–191
DOI 10.1007/s13538-012-0073-2

CONDENSED MATTER

Thallium Bromide Deposited Using Spray Coating

E. S. Ferreira · M. Mulato

Received: 17 January 2012 / Published online: 12 April 2012

Abstract Spray coating was used to produce thallium bromide samples on glass substrates. The influence of several fabrication parameters on the final structural properties of the samples was investigated. Substrate position, substrate temperature, solution concentration, carrying gas, and solution flow were varied systematically, the physical deposition mechanism involved in each case being discussed. Total deposition time of about 3.5 h can lead to 62-μm-thick films, comprising completely packed micrometer-sized crystalline grains. X-ray diffraction and scanning electron microscopy were used to characterize the samples. On the basis of the experimental data, the optimum fabrication conditions were identified. The technique offers an alternative method for fast, cheap fabrication of large-area devices for the detection of high-energy radiation, i.e., X-rays and γ-rays, in medical imaging.

Keywords TlBr · Thallium bromide · Film · Spray coating · Semiconductor · Radiation detector

1 Introduction

Solid-state physicists have contributed import advances to medicine concerning the interaction of radiation with matter and its detection. Examples are dosimeters and radiological detectors for applications in medical and dental imaging [1]. The benefits of digital medical imaging technique include appropriate acquisition, processing, and restoration of images, without the cost and problems associated with radiographic films [2]. In this field, the practical value of devices operational at room temperature has led to continuous efforts to develop wide-band gap semiconductors [3–7]. Equally valuable is the high stopping power of materials that interact strongly with ionizing radiation; large mass density is therefore desired [6]. Lead iodide [1, 8, 9], mercury iodide [10, 11], and thallium bromide [12–16] are among the most promising materials. Although crystals of these materials with millimetric bulk dimensions have been investigated for decades, few publications have dealt with films. The latter form is nonetheless fundamentally important in the medical imaging of ionizing radiation which requires large-area detectors, at the square meter scale [17]. And of course, industry would welcome cheaper and faster deposition techniques.

Thallium bromide (TlBr) has emerged as a particularly interesting semiconducting compound in view of its attractive features: large band gap (2.68 eV—2.5 times larger than Si), high mass density (7.56 g/cm^3—3.2 times larger than Si), and high atomic number (Tl 81 and Br 35) [6, 18–20]. TlBr has the CsCl crystalline structure and a relatively low melting point of 480°C [20–22]. These characteristics make it an excellent candidate for applications in room temperature X-ray and γ-ray detectors. Unfortunately, it is highly toxic and would hence have to be encapsulated.

Many researchers around the world are therefore looking for alternatives. Special attention has been given to methods that reduce the time of deposition of promising semiconductor films [2, 5, 17, 20, 23]. Currently, TlBr crystals are fabricated either by the Bridgeman–Stockbarger method or by the traveling molten zone method [6, 7, 12, 19]. TlBr films have been grown by thermal evaporation, but that process proved to be too slow for large-scale production [2, 8]. Alternative deposition techniques, ones combining

E. S. Ferreira · M. Mulato (✉)
Departamento de Física, FFCLRP-USP,
Av. Bandeirantes, 3900,
14040-9001 Ribeirão Preto, São Paulo, Brazil
e-mail: mmulato@ffclrp.usp.br

speed with low cost, are therefore needed. And since different structural and electrical properties may result from different techniques, a detailed analysis of each process seems warranted [24].

Here, we study the deposition mechanisms associated with spray coating of TlBr samples. Spray coating is a relatively cheap technique that can be easily expanded to large areas with the help of multiple spray nozzles and has recently been applied to develop other semiconducting candidates, such as PbI_2 [1, 9] and HgI_2 [10]. We discuss the structures of the resulting samples, associate them with the deposition parameters and physical deposition mechanisms during film growth, and suggest optimal deposition conditions.

2 Experimental Details

Thallium bromide samples were produced by a spray coating system. Our setup consists of a vacuum chamber with an electrically heated substrate holder at the bottom and a spraying system at the top. The single spraying nozzle has an internal diameter close to 260 μm. Nitrogen carries the spray. Thallium bromide is dissolved and stirred in DI water at 70°C, which is used as the starting solution after cooling down to room temperature. The solution was also filtered to prevent clogging of the spray nozzle. The flow of the solution is only started after reaching the desired nitrogen flux. The nitrogen and solution rates are controlled. They are mixed in the nozzle, and a spray is directed downwards toward the heated substrate. During deposition, Tl and Br atoms stick on top of the substrate, while water is evaporated. The process occurs under positive pressure, and the excess material is directed toward an outer water reservoir before being ejected to a hood. The starting (low) vacuum, before deposition, is around 0.335 bar. The maximum substrate temperature is 300°C. Solutions were prepared with 0.05 g of commercial TlBr (Merck, 99.0 %) diluted in 100, 150, and 200 g of DI water. Glass substrates, 1.0×2.5 cm^2, were prepared according to standard glass cleaning procedures.

Our study of the influence of the central deposition parameters on the final structure of the obtained samples is based on X-ray diffraction (XRD) and scanning electron microscopy (SEM). The structural characterization of the samples used Cu K_α radiation from a Siemens D5005 (40 kV/40 mA) diffraction system. The scanning angle (2θ) was varied from 2° to 70°, with a step of 0.02°/s. An LED-440 scanning electron microscope examined the surface of the samples.

3 Results and Discussions

Figure 1 shows the typical XRD pattern of the TlBr samples. In this specific case, the samples resulted from 12 mL/h flow of

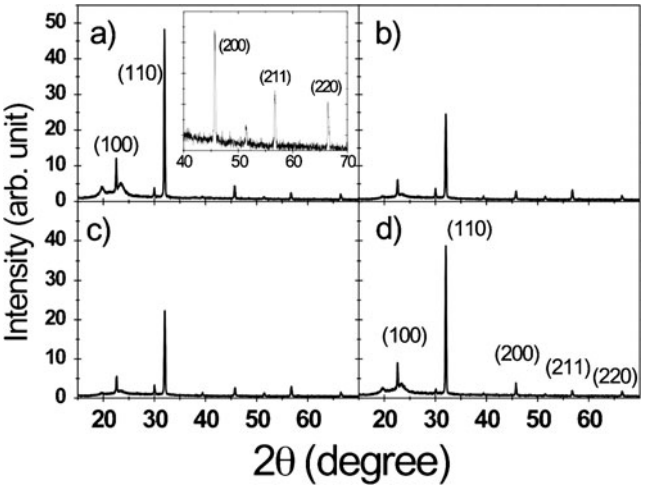

Fig. 1 XRD data for samples deposited during 2 h at 100°C using a total saturated solution volume of 50 mL and nitrogen flow of 10 L/min. *a–d* correspond to substrates aligned along the diameter of the substrate holder at positions 1 to 4, respectively. The *inset* in *a* shows the high-angle region in more detail

50 mL saturated solution and 10 L/min nitrogen flow. The glass substrates corresponding to diffractograms (a)–(d), identified by the numbers 1–4, respectively, were linearly accommodated along the diameter of the substrate holder. Total deposition time was 2 h, the substrate temperature kept at 100°C. The most intense diffraction peak, corresponding to the (110) plane, and less intense ones were identified on the basis of the JCPDS-8-486 data. The data in the figure suggest that the external substrates 1 and 4 yield more intense peaks. This may be due to more deposition of material or to more crystalline samples at the borders, or even to a combination of the two effects. In fact, to a large extent, the final structure is determined by the conical shape of the spray inside the chamber.

The influence of the spray geometry depends on the deposition parameters. As an illustration, Fig. 2 presents a more detailed analysis of the XRD data for three nitrogen flows ranging from 6 to 10 L/min, the other deposition parameters kept unchanged relative to Fig. 1. Figure 2 a presents the total integrated area of the XRD spectra for each flow rate. The triangles corresponding to the flow rate in Fig. 1, the integrated intensities for substrates 1 and 4 are larger than for substrates 2 and 3. Depending on the homogeneity of the spray, two explanations can be inferred from the data: (a) If the spray is homogeneous, a nitrogen flow of 10 L/min may be too strong, so that near the substrate holder, due to backscattering, some TlBr material is not deposited; or (b) if the spray is not homogeneous and nitrogen is dominant near the center, the concentration of TlBr material increases with radius, causing more material to be deposited at the most external substrates. Either hypothesis is consistent with the progressively more uniform integrated intensities as the nitrogen flow is reduced in the upper curves in Fig. 2 a.

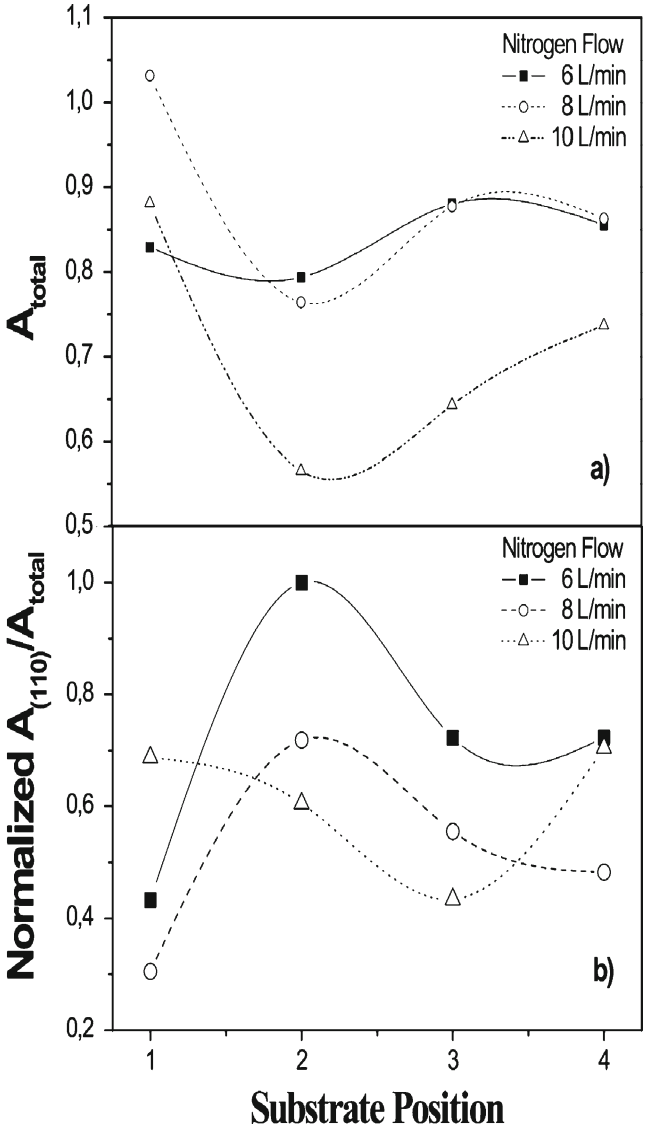

Fig. 2 a Total integrated area of the XRD spectra for three deposition conditions using a nitrogen flows ranging from 6 up to 10 L/min as a function of the substrate position, labeled as in Fig. 1. The other deposition parameters reproduce the conditions described in Fig. 1. *b* Ratio of the integrated area of the (110) XRD peak to the total area under XRD pattern as a function of substrate position. For easier comparison, all the final data were normalized to the integrated area of the substrate at position number 2 with 6 L/min nitrogen flow rate. The *lines* are guides to the eyes

More detailed analysis reveals that the results in Figs. 1 and 2 a are only partially due to unequal amounts of deposited material. Crystallinity also plays an important role. Figure 2 b presents the ratio of the integrated area of the (110) XRD peak to the total area of the corresponding X-ray diffractogram. For easier comparison, all data were normalized with respect to substrate number 2 under the 6 L/min nitrogen flow. While for 10 L/min nitrogen flow, the material at the borders (substrates 1 and 4) is more crystalline, the smaller nitrogen flow rates give rise to less crystalline films at the borders. Not only does the position at which the material is most crystalline change with the nitrogen flow rate: As the nitrogen rate is reduced, there is an overall improvement of crystallinity.

The total deposition time is an important parameter. Increased deposition times tend to increase the substrate coverage and the film thickness. Since the formation of water droplets in the inner top of the chamber in practice limits the deposition time, we heated the system externally to keep the top part of the chamber at 48°C and avoid condensation. Longer deposition times could then be achieved, even with higher solution flows.

The substrate temperature is another important deposition parameter. Since the carrying liquid is water, the substrate must be kept at 100°C or above, the data in Figs. 1 and 2 corresponding to the lower-temperature limit of the technique. We have investigated the influence of substrate temperature up to 300°C. We fixed the nitrogen flow at 10 L/min and studied two different solutions: 50 mg of TlBr dissolved in either 100 or 200 mL of water. A larger solution flow, 27 mL/h, was used during 2 h. Since these experiments were performed almost in parallel with the ones described in Figs. 1 and 2, the above-discussed conclusions had no influence on our choice of nitrogen flow.

Figure 3 presents the XRD results for the more concentrated solution. All the data correspond to the most crystalline sample under these deposition conditions, for fixed substrate position. The intensities of the crystalline peaks decrease with increasing substrate temperature. Figure 3 f shows that, notwithstanding the different concentrations, both solutions display the same trend. As spelled out by the following argument, this indicates that the substrate spits part of the deposited material.

During spray coating, the carrying liquid and salt particles of the original solution reach the substrate. The liquid is expected to thermally evaporate, leaving the salt particles to form the final film. The higher the temperature of the substrates, the more energetic are the evaporated water molecules, part of which can scatter the incoming salt particles away from the substrate and hence reduce the deposition rate.

An alternative explanation considers the effects of the temperature gradient inside the chamber. Before deposition, the substrate temperature is set to the desired value. Nitrogen flow is adjusted, and a positive pressure is established inside the chamber. Only then is the flow of solution started. The spray nozzle is roughly 17 cm away from the substrate, while the diameter of the cylindrical chamber is close to 15 cm, leading to an approximately unitary aspect ratio. As already discussed, only the top surface of the chamber is heated to avoid condensation of water molecules, the temperature of the lateral wall being neither controlled nor monitored. Early in the deposition, the wall is close to room

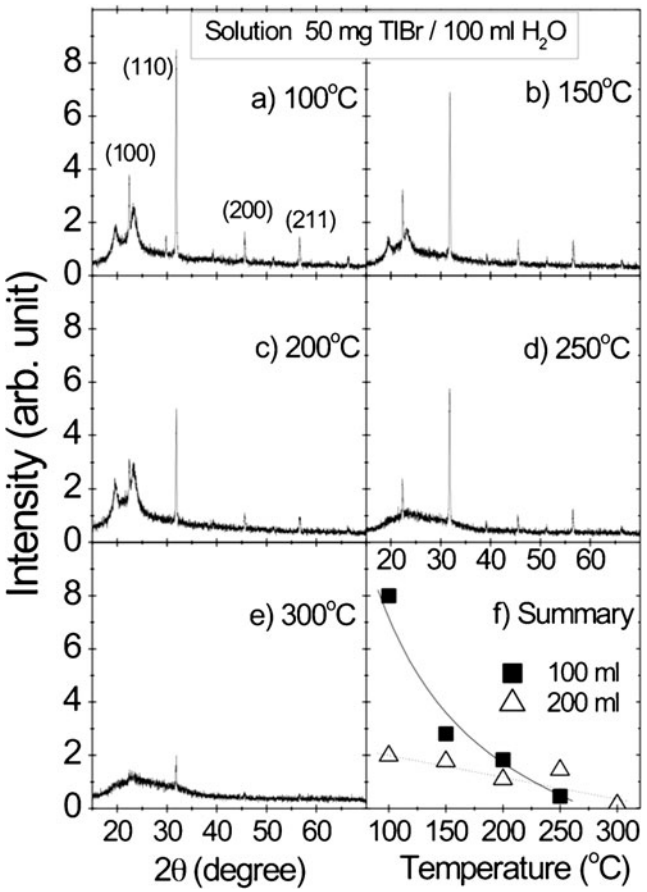

Fig. 3 XRD data for samples deposited at the indicated substrate temperatures. A solution concentration of 50 mg TlBr diluted in 100 mL H_2O was used, with 27 mL/h solution flow, 10 mL/min gas flow, and 2.0 h total deposition time. From *a* to *e*, the higher the temperature, the smaller the intensity of the crystalline diffraction peak. *f* The intensity of the main peak (110) for two dilutions, the same amount of powder being solved in 100 or 200 mL water. The drop is more pronounced for the more concentrated solution (*filled squares*)

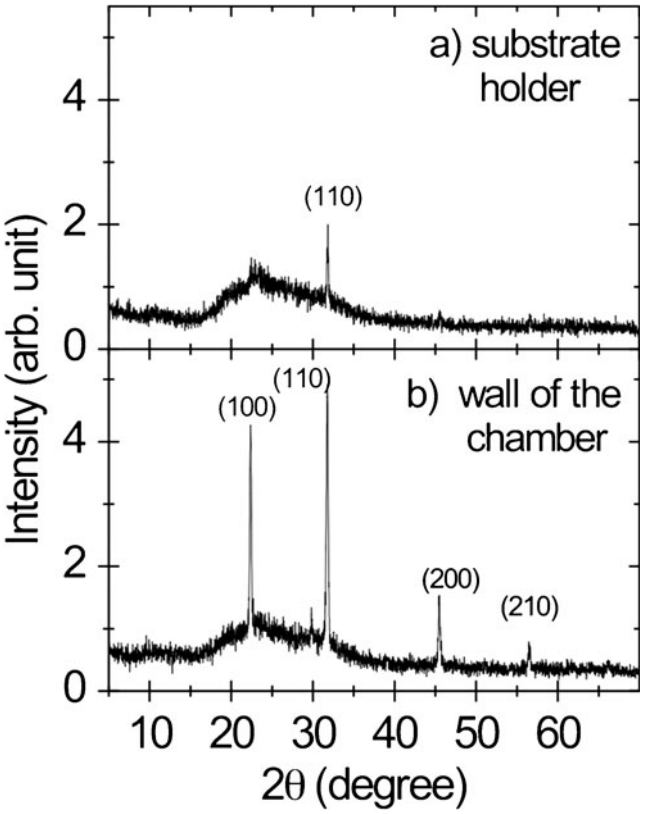

Fig. 4 XRD data for samples fabricated under the deposition conditions in Fig. 3. *a* The diffractogram for a sample deposited on the substrate holder and *b* for a sample deposited at the lateral wall of the chamber

temperature, i.e., well below the substrate temperature. A temperature gradient is therefore likely to develop inside the chamber. This gradient would distort the path of the salt particles after the solution starts to flow, since the salt particles would be preferentially directed toward places at lower temperatures.

Either of these two explanations leads to the conclusion that some material is deposited off the substrate holder; at the highest temperatures, film may even be deposited at the lateral wall. The higher the substrate temperature, the smaller the amount of material on the substrates and higher the amount of material scattered elsewhere. This conclusion is also consistent with Fig. 3 f, which associates a more pronounced effect with the heavier flow of salt particles produced by the more concentrated solution.

In order to prove our point, Fig. 4 compares the XRD data from two samples fabricated in the same run. The substrate was heated to 300°C, and the deposition parameters reproduce the conditions under which Fig. 3 e was generated. Figure 4 a corresponds to a sample deposited on top of the substrate holder, while Fig. 4 b corresponds to a sample deposited on a substrate attached to the inner lateral wall of the system, vertically aligned with the substrate holder. Clearly, in agreement with the previous discussion, more material is deposited at the wall than at the position of the holder.

The relative intensities of crystalline peaks in Fig. 4 b are nonetheless different from the pattern in the diffractograms in Figs. 1 and 3. For instance, the intensities of the (100) and

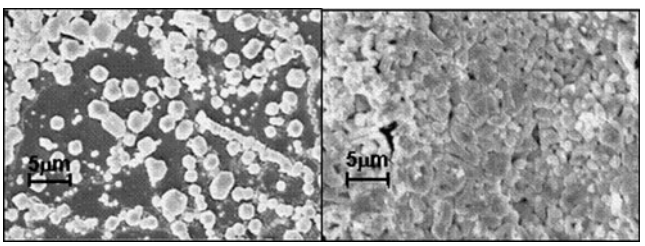

Fig. 5 SEM photographs for samples deposited under different conditions. **a** Solution flow of 27 mL/h and total deposition time of 2.0 h; **b** solution flow of 51 mL/h and total deposition time of 3.5 h. More material was therefore deposited for longer time in **b**. Both samples were produced at 100°C, with 10 L/min nitrogen flow

(110) peaks are approximately the same. Given that the substrate at the wall is close to room temperature, i.e., well below 100°C, we conclude that lower temperatures lead to less oriented or more polycrystalline material. This is easy to understand, since adatoms deposited on colder substrates have smaller surface mobility.

In summary, higher temperatures yield thin films of inferior quality. The optimum substrate temperature is slightly above the thermal evaporation point of the solvent. This less aggressive process may prove valuable in subsequent development of films for technological applications.

Figure 5 presents SEM photographs of sample surfaces, which monitor the evolution of the substrate coverage. The samples were prepared with predefined total deposition times and solution flow rates. Figures 5a, b correspond total deposition times (solution flow rates) of 2.0 and 3.5 h (27 and 51 mL/h), respectively. In the second case, more material is thus deposited for longer time. Both samples were produced at 100°C, with 10 L/min nitrogen flow. Figure 5a clearly shows that the film is not formed in a layer by layer process. In fact, crystalline grains start to develop at random regions of the substrate. Dark regions most probably correspond to the glass substrate. Complete coverage is only obtained after longer deposition times, as shown by Fig. 5b. Even in this case, it can be clearly seen that the final sample corresponds to a film comprising an arrangement of packed crystalline grains. The final thickness of this sample, measured by cross-sectional SEM, is 62 μm, corresponding to a deposition rate of approximately 18 μm/h. This rate is compatible with technological demands. The observed grain distribution may, however, prove inadequate for technological devices based on electronic transport and hence calls for additional investigation.

4 Conclusion

Thallium bromide films were produced using spray coating, with water as solvent of the original salt. The characterization of the resulting films recommends a saturated solution to optimize the deposition. The top surface of the chamber must moreover be heated to avoid internal condensation of evaporated water molecules. The resulting films are oriented along the (110) plane. The distribution of deposited material on the substrate holder area depends on the carrying-gas flow rate. With increasing flow rate, more material is deposited on the outer regions, and the resulting mass distribution profile over the substrate holder changed from convex to concave. This finding opens opportunities for future uses of multiple spray nozzles to cover large areas as required by the fabrication of medical detectors.

Our results recommend a substrate temperature close to the point of evaporation of the solvent, which defines the least aggressive process. Higher substrate temperatures reduce the amount of deposited material, either due to spitting collision or to a temperature gradient inside the chamber. The adatoms are not deposited layer by layer; instead, individual crystals grow randomly. Complete coverage, with 62 μm thickness, corresponding to a deposition rate of 18 μm/h, is obtained after deposition times as long as 3.5 h. On the basis of the standard defined by these parameters, samples can be easily produced, additional study of which these parameters provide a standard, on the basis of which samples can be produced and additionally studied for practical purposes such as the fabrication of large-area radiation detectors.

Acknowledgments We thank C. A. Brunello, Dr. J. C. Ugucioni, Prof. M. M. Hamada, Prof. J. F. Condeles, and Prof. M. Ferreira for experimental help. This work has been funded by CAPES, FAPESP, and CNPq Brazilian agencies.

References

1. J.F. Condeles, R.A. Ando, M. Mulato, Optical and structural properties of PbI2 thin films. J. Mater. Sci. **43**, 525–529 (2008)
2. P.R. Bennett, K.S. Shah, L.J. Cirignano, M.B. Klugerman, L.P. Moy, F. Olschner, M.R. Squillante, Characterization of polycrystalline TlBr films for radiographic detectors. IEEE Trans. Nucl. Sci. **46**, 266–270 (1999)
3. L.X. Li, F.Y. Lu, C. Lee, G. Wright, D.R. Rhiger, S. Sen, K.S. Shah, M.R. Squillante, L.J. Cirignano, B.B. Ralph, A. Burger, P. Luke, R. Olson, Development of large single crystal (3-inch ingots) CdZnTe for large volume nuclear radiation detectors. X-Ray Gamma-Ray Detect. Appl. IV **4784**, 76–83 (2002)
4. M. Amman, J.S. Lee, P.N. Luke, Alpha particle response characterization of CdZnTe, hard X-ray and gamma-ray detector physics III. Proc. Soc. Photo-optical Instrum. Eng. (SPIE) **4507**, 1–11 (2001)
5. K. Hitomi, O. Muroi, T. Shoji, T. Suehiro, Y. Hiratate, Room temperature X- and gamma-ray detectors using thallium bromide crystals. Nucl. Inst. Methods Phys. Res. A—Accel. Spectrom. Detect. Assoc. Equip. **436**, 160–164 (1999)
6. P.J. Sellin, Recent advances in compound semiconductor radiation detectors. Nucl. Inst. Methods Phys. Res. A—Accel. Spectrom. Detect. Assoc. Equip. **513**, 332–339 (2003)
7. I.B. Oliveira, F.E. Costa, J.F.D. Chubaci, M.M. Hamada, Purification and preparation of TlBr crystals for room temperature radiation detector applications. IEEE Trans. Nucl. Sci. **51**, 1224–1228 (2004)
8. L. Fornaro, E. Saucedo, L. Mussio, L. Yerman, X. Ma, A. Burger, Lead iodide film deposition and characterization. Nucl. Inst. Methods Phys. Res. A—Accel. Spectrom. Detect. Assoc. Equip. **458**, 406–412 (2001)
9. J.F. Condeles, M. Mulato, Influence of solution rate and substrate temperature on the properties of lead iodide films deposited by spray pyrolysis. J. Mater. Sci. **46**, 1462–1468 (2011)
10. J.C. Ugucioni, M. Mulato, Influence of deposition temperature, solvent and solute concentration on the deposition mechanisms and final structure of mercury iodide fabricated using the spray pyrolysis technique. J. Appl. Phys. **100**, 043506 (2006)
11. A.R. Rao, V. Dutta, V.N. Singh, Multiwalled HgX (X = S, Se, Te) nanotubes formed with a mercury iodide catalyst in nanocrystalline

thin films spray-deposited at low temperature. Adv. Mater. **20**, 1945–1951 (2008)
12. I.B. Oliveira, J.F.D. Chubaci, M.J.A. Armelin, M.M. Hamada, Purification and crystal growth of TlBr for application as a radiation detector. Cryst. Res. Technol. **39**, 849–854 (2004)
13. K. Hitomi, Y. Kikuchi, T. Shoji, K. Ishii, Improvement of energy resolutions in TlBr detectors. Nucl. Inst. Methods Phys. Res. A—Accel. Spectrom. Detect. Assoc. Equip. **607**, 112–115 (2009)
14. K. Hitomi, Y. Kikuchi, T. Shoji, K. Ishii, Evaluation of TlBr detectors with Tl electrodes. Hard X-Ray Gamma-Ray Neutron Detect. Phys. X **7079**, J790 (2008)
15. N. Destefano, M. Mulato, Influence of multi-depositions on the final properties of thermally evaporated TlBr films. Nucl. Inst. Methods Phys. Res. A—Accel. Spectrom. Detect. Assoc. Equip. **624**, 114–117 (2010)
16. N. Destefano, M. Mulato, Thermally evaporated thallium bromide films fabricated at varied substrate temperatures. J. Mater. Sci. **46**, 2229–2234 (2012)
17. K. Hitomi, O. Muroi, M. Matsumoto, T. Shoji, Y. Hyratate, Large-volume thallium bromide detectors for gamma-ray spectroscopy. IEEE Trans. Nucl. Sci. **48**, 2313–2316 (2001)
18. A. Owens, M. Bavdaz, G. Brammertz, V. Gostilo, H. Graafsma, A. Kororezov, M. Krumrey, I. Lisjutin, A. Peacock, A. Puig, H. Sipila, S. Zatoloka, The X-ray response of TlBr. Nucl. Inst. Methods Phys. Res. A—Accel. Spectrom. Detect. Assoc. Equip. **497**, 370–380 (2003)
19. A. Owens, M. Bavdaz, G. Brammertz, V. Gostilo, N. Haack, A. Kororezov, I. Lisjutin, A. Peacock, S. Zatoloka, Hard X-ray spectroscopy using a small-format TlBr array. Nucl. Inst. Methods Phys. Res. A—Accel. Spectrom. Detect. Assoc. Equip. **497**, 359–369 (2003)
20. K. Hitomi, O. Muroi, M. Matsumoto, R. Hirabuki, T. Shoji, T. Suehiro, Y. Hiratate, Recent progress in thallium bromide detectors for X- and gamma-ray spectroscopy. Nucl. Inst. Methods Phys. Res. A—Accel. Spectrom. Detect. Assoc. Equip. **458**, 365–369 (2001)
21. K.S. Shah, J.C. Lund, F. Olschner, L. Moy, M.R. Squillante, Thallium bromide radiation detectors. IEEE Trans. Nucl. Sci. **36**, 199–201 (1989)
22. K. Hitomi, M. Matsumoto, O. Muroi, T. Shoji, Y. Hiratate, Characterization of thallium bromide crystals for radiation detector applications. J. Cryst. Growth **225**, 129–133 (2001)
23. K. Hitomi, O. Muroi, T. Shoji, Y. Hiratate, H. Ishibashi, M. Ishii, Thallium bromide photodetectors for scintillation detection. Nucl. Inst. Methods Phys. Res. A—Accel. Spectrom. Detect. Assoc. Equip. **448**, 571–575 (2000)
24. R.J.M. Konings, E.H.P. Cordfunke, J.E. Fearon, R.R. Vanderlaan, The infrared spectrum and vapour pressure of lead diiodide. Thermochim. Acta **273**, 231–238 (1996)